International Journal of Applied Engineering Research ISSN 0973-4562 Volume 10, Number 24 (2015) pp 44939-44947

Modeling Dust Particle Dynamics In Suction Units With Rotating Cylinders

Olga A. Averkova, Artur K. Logachev, Valeryi A.Uvarov
Belgorod State Technological University named after V.G.Shoukhov,
Russia, 308012, Kostykova str., 46,

Abstract- The article investigates the behavior of dust particles of different shapes and densities in closed local ventilation exhausts (aspiration shelters). There are proposed measures to reduce dust discharge in the aspiration network. To describe the behavior of dust particles in swirling air flows developed a method of mathematical modeling and a computer program. Obtained results can be used for designing of local ventilation exhausts of closed type with the function of dust precipitation chamber. The maximum diameter of the dust particles, entrained into an aspiration network of local ventilation exhausts of closed type (aspiration shelters), taking into account intake of air through leakages, essentially depends on bounding visors, availability of rotating cylinders and exhaust-cylinders. Geometrical dimensions of mechanical screens and cylinders, their location, the linear speed of rotation of the latter were determined, contributing to the reduction of the maximum diameter aspirated of dust particles on 140-200 microns.
Keywords: Aspiration, method of boundary integral equations, rotating cylinders, dust particles.

Introduction

Maximum diameter d_{max} of dust particles carried over into the suction system from hoods that contain dust emissions from various processes is needed to be determined for the purpose of a scientifically grounded choice of dust collecting equipment [1,2]. According to the hypothesis by Professor V.A. Minko [3] using the maximum diameter value it is possible to forecast the particle size distribution. This hypothesis was proven to be correct by pilot tests conducted for suction units of various design in transfer of bulk materials [3,4-8].

There was the flight of round-shaped dust particles previously studied. As compared to the experimental data the design maximum diameter of dust particle was lower for 50-70 μm [4].

In addition, for practical purposes it is reasonable to decrease the suction system dust losses and use a suction unit as a settling chamber to reduce exhaust air treatment costs. For instance, there is a partition installed inside a hood along with chain curtains to reduce dust losses. Or, as we have already suggested, a rotating suction cylinder can be installed inside a hood.

Therefore, this article objective is to determine d_{max} of finely dispersed aerosols of various physical properties carried over into the suction system and to elaborate constructive solutions as to design of suction units with settling chamber functions.

Materials and Methods

Let a multiply connected flow region be limited by boundary *S* on which the normal velocity is given as function of coordinates and time $v_n(x_0,t)$ where $x_0 \in S$. There may be impermeable cylinders (denoted by circles) within the region rotating at linear velocities v_i. We'll assume that there are sources (outflows) of $q(\xi,t)$ intensity unknown in advance distributed continuously along the boundary. Let linear vortexes be located in the cylinder centers $a_i(a_{i1},a_{i2})$ with circulations $L_i = 2\pi r_i \cdot v_i$, where r_i is *i* cylinder radius. The impact of all these sources (outflows) and vortexes on inner point *x* of the flow area will be given by the integral equation:

$$v_n(x,t) = \int_S F(x,\xi)q(\xi,t)dS(\xi) + \sum_{i=1}^{m} L(a_i)G(x,a_i),$$

where $v_n(x,t)$ is the velocity at point $x(x_1,x_2)$ along $\vec{n} = \{n_1,n_2\}$ at the instant of time *t*; *m* is the number of rotating cylinders;

$$F(x,\xi) = \frac{n_1(x_1-\xi_1)+n_2(x_2-\xi_2)}{2\pi\left[(x_1-\xi_1)^2+(x_2-\xi_2)^2\right]};$$

$$G(x,a_i) = \frac{n_2(x_1-a_{i1})-n_1(x_2-a_{i2})}{2\pi\left[(x_1-a_{i1})^2+(x_2-a_{i2})^2\right]}; \quad dS(\xi)$$

means that the integration variable is ξ.

Letting inner point to boundary point x_0 along the outward normal we have the boundary integral equation:

$$v_n(x_0,t) = -\frac{1}{2}q(x_0,t) + \int_S F(x_0,\xi)q(\xi,t)dS(\xi) + \sum_{i=1}^{m} L(a_i)G(x_0,a_i), \quad (1)$$

where the first term results from calculation of the integral singularity at $x_0 = \xi$, therefore the integral itself does not contain this point.

By discretizing the region boundary into *N* boundary intervals at each of which intensity $q(\xi,t)$ will be assumed to be constant we'll obtain a discrete countertype of (1):

$$v_n^p = -\frac{1}{2}q^p + \sum_{\substack{k=1,\\ k\neq p}}^{N} q^k F^{pk} + \sum_{i=1}^{m} L_i G_i^p$$

where $v_n^p = v_n(x_0^p,t)$; x_0^p is the middle of *p* interval; $q^p = q(x_0^p;t)$; $q^k = q(\xi^k,t)$; ξ^k is a random pint of *k* interval; $F^{pk} = \int_{\Delta S^k} F(x_0^p,\xi^k)dS(\xi^k)$ is an integral over *k* interval; $L_i = L(a_i)$, $G_i^p = G(x_0^p,a_i)$.

Searching through *p* values from 1 to *N* we have a set of *N* linear algebraic equations with *N* unknown variables solving which we'll find intensities of sources (outflows) q^1, q^2, ..., q^N at the given instant of time *t*. Accordingly, the required velocity at inner point *x* will be determined from the formula:

$$v_n(x) = \sum_{k=1}^{N} q^k F^k + \sum_{i=1}^{m} L_i G_i,$$

Where $F^k = \int_{\Delta S^k} F(x,\xi^k)dS(\xi^k)$;

$$G_i = G(x,a_i). \quad (3)$$

In order to plot the flow line it is required to set an initial point, calculate horizontal (v_x) and vertical (v_y) air velocity components at this point thus having defined flow direction $\vec{v}$; take a step in this direction and repeat the calculation procedure set forth above. The reverse calculation procedure is also possible when the flow line is plotted from the suction port, i.e. a step is taken in the direction opposite to vector $\vec{v}$. The calculation stops as soon as the air exhaust line is reached or as the flow line length exceeds the given value.

A dust particle path is plotted based on the following motion equation integration using the Runge-Kutta method:

$$\rho_1 \frac{\pi d_e^3}{6} \cdot \frac{d\vec{v}_1}{dt} = -\psi \cdot \frac{|\vec{v}_1 - \vec{v}|(\vec{v}_1 - \vec{v})}{2} \rho\chi S_m + \rho_1 \frac{\pi d_e^3}{6}\vec{g}$$

, where ρ_1, ρ are dust particle and medium densities respectively; $\vec{v}_1$ is the particle velocity vector; $\vec{v}$ is the air velocity calculated from formula (3); d_e is an

equivalent diameter; $S_m = \pi d_e^2/4$ is the transparent frontal area; χ is the particle dynamic form-factor; $\vec{g}$ is the gravity factor; ψ is the drag factor:

$$\psi = 24/\mathrm{Re} \quad \text{at} \quad \mathrm{Re} < 1;$$

$$\psi = 24\left(1 + 1/6 \cdot \mathrm{Re}^{2/3}\right)/\mathrm{Re} \quad \text{at} \quad 1 \le \mathrm{Re} < 10;$$

$$24/\mathrm{Re} \cdot \left(1 + 0{,}065\,\mathrm{Re}^{2/3}\right)^{1.5} \quad \text{at} \quad \mathrm{Re} \ge 10^3.$$

When a particle is hitting a solid wall tangential ($v_{2\tau}$) and normal (v_{2n}) velocities are calculated from the formula:

$$v_{2n} = -k \cdot v_{0n}, \quad v_{2\tau} = v_{0\tau} + \eta \cdot f \cdot (1+k) \cdot v_{0n},$$

where $\eta = \min\left\{-\frac{2v_{0\tau}}{7 f (1+k) v_{0n}}, 1\right\}$; k is the coefficient of restitution ; f is the coefficient of sliding friction.

When dust particle paths are calculated in a region with time-variant boundary conditions in order to determine the air velocity the intensity of sources (outflows) distributed along the flow boundary must be recalculated at each instant of time by solving set (2).

There was Spectrum [8] software program developed based on the algorithms described above to enable determining the field of velocities, plotting flow lines and paths of dust particles in multiply connected regions with complex boundaries where the normal velocity component may vary in time and where the given number of rotating cylinders can be present.

Let us analyze a hood used in transfers of bulk materials (Fig. 1) studied in industrial conditions [4-7]. We'll determine the maximum diameter of dust particles carried over into the suction system.

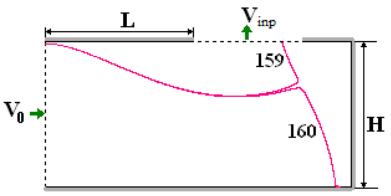

Fig. 1. Paths of dust particles in suction units

Results and Discussion

The hood under analysis (Fig. 2) is used for containment of dust emissions from a conveyor feed unit at ore preparation plants.

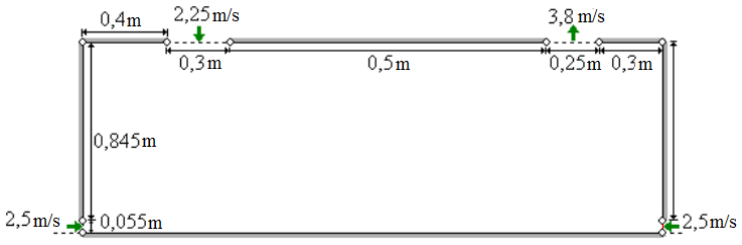

Fig. 2. Single-wall hood

With increase in the initial vertical escape velocity of a dust particle (downward) having the density of 3500 kg/m^3 the maximum diameter is decreased for 10-25 μm (Fig. 3).

We'll assume hereinafter that a dust particle escape velocity is equal to the inlet air flow velocity (2.25 m/s).

With increase in the dust particle dynamic form-factor and decrease in the dust particle density the maximum diameter of such particle significantly increases. (Fig. 4).

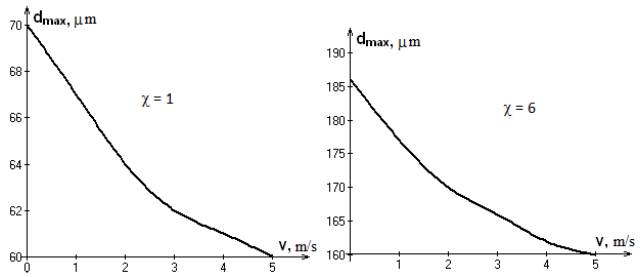

Fig. 3. Maximum diameter vs. initial escape velocity of dust particle

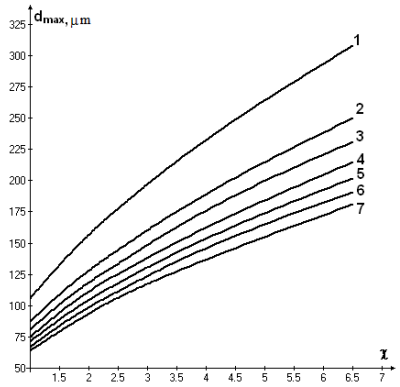

Fig. 4. Maximum diameter vs. form-factor and density of dust particle: 1 – 1400 kg/m^3, 2 – 2000 kg/m^3, 3 – 2300 kg/m^3, 4 – 2600 kg/m^3, 5 – 2900 kg/m^3, 6 – 3200 kg/m^3, 7 – 3500 kg/m^3

Let us analyze the relation of d_{max} from the screen location (Fig. 5) and length. Geometrical and aerodynamic characteristics of the hood are the same as on Fig. 2.

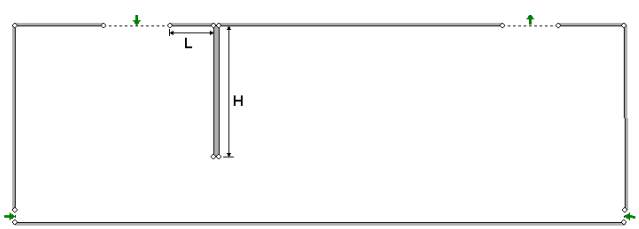

Fig. 5. Double-wall hood

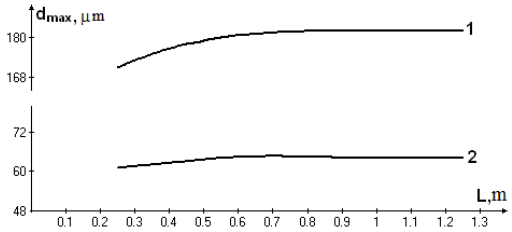

Fig. 6. Relation of d_{max} to the screen distance from the inlet if its length H = 0.4 m and dust particle density of 3500 kg/m^3: 1- χ = 6.5; 2 - χ = 1

If the screen is displaced from the inlet to the outlet d_{max} will be virtually constant. A very slight decrease in this value can be observed if the screen is at a distance of less than 0.5 m (Fig. 6).

The analysis of calculations shown on Fig. 7 demonstrates that the greatest decrease in the dust particle maximum diameter for 10-15 μm is observed when the screen is positioned at distance L=0.25 m from the inlet. The numeric characters shown on the figures describe the density of dust particles as well as shown on Fig. 4.

If a dust particle escape velocity is changed d_{max} remains the same. For instance, if there is a spherical dust particle having the density of 3500 kg/m^3 and the velocity variation is between 0 and 5 m/s, screen length H = 0.55 m and the distance between the screen and the inlet L=0.25 m, then d_{max} = 54 μm.

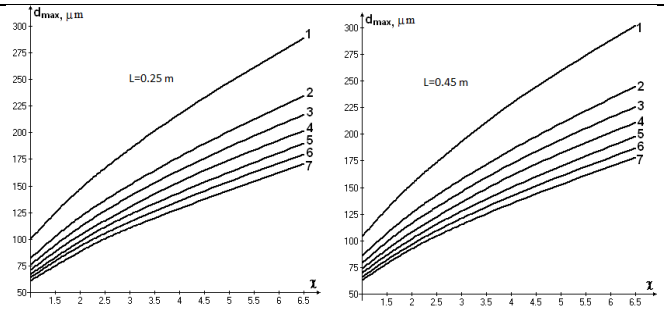

Fig. 7. Relation of d_{max} to dust particle form-factor and density if H = 0.4 m

The screen length has a great impact on d_{max} (Fig. 8). If H is increased from 0.3 m to 0.5 m d_{max} will be decreased for 8-21 μm based on the dynamic form-factor.

In all calculations hereinafter the initial point of dust particle escape will be in the rightmost inlet position which is due to the fact that this point is the closest one to the outlet and the maximum diameter value will be the greatest in such case.

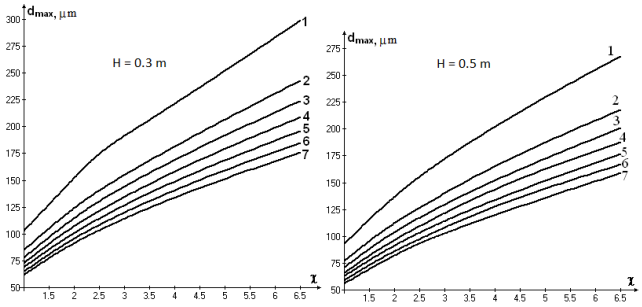

Fig. 8. Relation of d_{max} to dust particle form-factor and density if L=0.25 m

We'll analyze dust dynamics in a double-wall suction unit with a rotating cylinder installed inside. All other geometric and kinematic parameters are the same as for the hood shown on Fig. 2. The screen distance L and length H were chosen based on the conditions most favored for reduction in the maximum diameter of a dust particle carried over into the suction system and based on the technological conditions (Fig. 9).

As it was shown by the numerical experiment the best cylinder position is below the screen. With decrease in the cylinder radius d_{max} is increased. The radius chosen for the study is 0.1 m which is stipulated by the technological conditions: there should be a distance between the cylinder and the belt conveying a bulk material sufficient to pass the material. The air flow induced by the cylinder rotation should be expected to contribute to settlement of dust particles on the hood bottom.

During clockwise rotation of the cylinder the maximum diameter is slightly greater than in case with counterclockwise rotation however there is a number of interesting phenomena observed. The air flow induced by the cylinder affects most the flight of fine particles. Therefore, fine particles entrained at the right of the cylinder are settling within some range (Fig. 10). With further decrease in the preset dust particle diameter particles are flying around the cylinder, escaping into the slot between the cylinder and the screen to be further carried over into the suction port. It should be also noted that all dust particles are escaping into the space beyond the screen only though the slot between the cylinder and the screen where the velocity is rather high (e.g. about 35 m/s for Fig. 10).

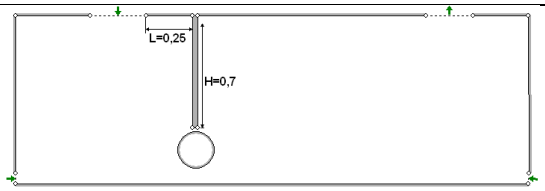

Fig. 9. The model of a double-wall hood equipped with a rotating cylinder

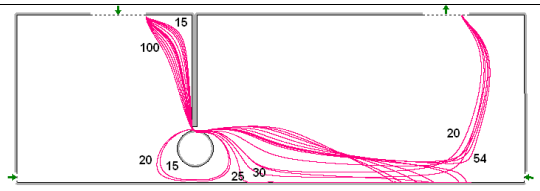

Fig. 10 Paths of dust particles having the density of 3500 kg/m^3 and χ = 1.83 when the cylinder is rotating clockwise at the linear velocity of 8 m/s

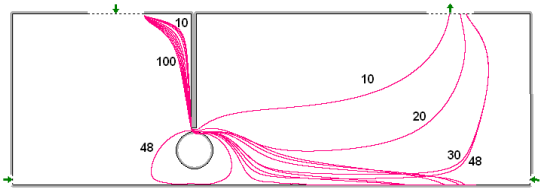

Fig. 11. Paths of dust particles having the density of 3500 kg/m^3 and χ = 6.5 when the cylinder is rotating clockwise at the linear velocity of 8 m/s

The pattern of paths for plate-like dust articles is somewhat different (Fig. 11). There is no intermediate fraction that would settle on the hood bottom. The maximum diameter here (Fig. 12) is lower than in case with counterclockwise rotation of the cylinder.

However, in our view, no particle size distribution can be forecasted by d_{max} when the cylinder is rotating clockwise. There will be no logarithmic normal distribution of dust particles here since some intermediate fractions are settling on the hood bottom.

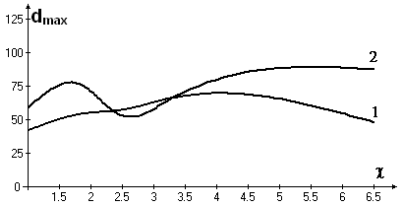

Fig. 12. Relation of d_{max} (μm) to form-factor χ when the cylinder is rotating clockwise at the linear velocity of 8 m/s with the dust particle density of: 1 – 3500 kg/m^3; 2 – 1400 kg/m^3

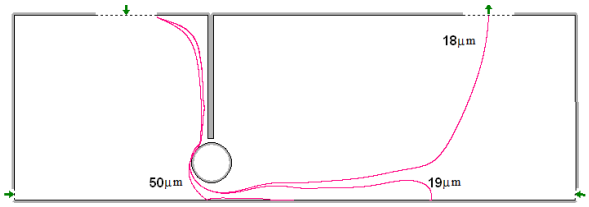

Fig. 13. Paths of ball-shaped dust particles having the density of 3500 kg/m^3 when the cylinder is rotating counterclockwise at the linear velocity of 5 m/s

During counterclockwise rotation of the cylinder (Fig. 13) the air flow induced by the cylinder contributes to precipitation of particles. At low rotation velocities (up to 2 m/s) the point where particles collide with the cylinder is near the screen and a bounced dust particle takes the direction that contributes to the particle being carried over by the air flow between the cylinder and the screen towards the exhaust outlet. This explains an increase in d_{max} as respects the case with a resting cylinder (Fig. 14-15). With increase in the cylinder rotation velocity the bouncing point is displaced counterclockwise and at definite rotation velocities a dust particle is clearing the cylinder to settle on the hood bottom or is flying between the

cylinder and the bottom. Note that the flow between the cylinder and the screen also changes its direction. In this case d_{max} will be decreased. Starting from the cylinder rotation velocity of over 4 m/s such decrease is insignificant (Fig. 14-15).

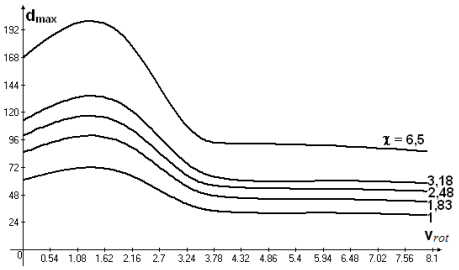

Fig. 14. Relation of d_{max} to the cylinder counterclockwise rotation velocity
with the dust particle density of 3500kg/m^3

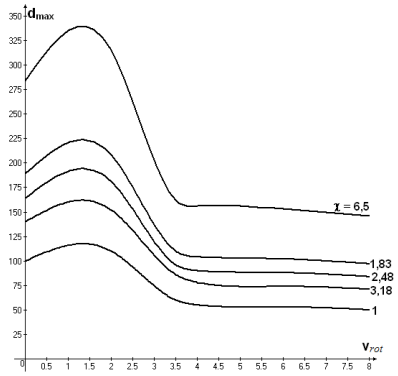

Fig. 15. Relation of d_{max} to the cylinder counterclockwise rotation velocity
with the dust particle density of 1400kg/m^3

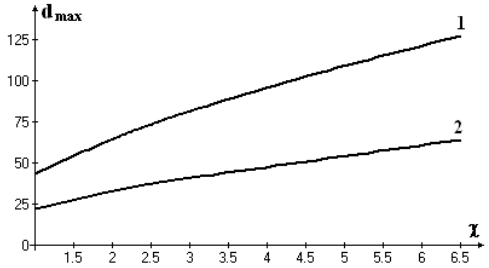

Fig. 16. Relation of d_{max} (μm) to form-factor χ during the counterclockwise rotation
of the cylinder centered on (1,97; -1,05) at the velocity of 8 m/s and with dust particle density of 1 – 1400kg/m^3; 2 – 3500kg/m^3

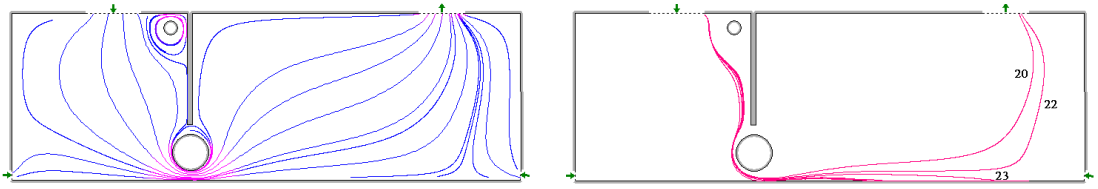

a) b)

Fig. 17. The hood equipped with two cylinders rotating counterclockwise at the velocity of 8 m/s: a) flow lines; b) paths of ball-shaped dust particles having the density of 3500 kg/m^3

Note that when the cylinder is lowered the maximum diameter is decreased (Fig. 16). The best position of the cylinder is (1.97;-1.05). Here the relation of dmax to □ is actually linear.

When the second cylinder rotating counterclockwise is installed in the corner between the screen and the inflow wall (Fig. 17) the maximum diameter decrease effect is even clearer. It should be noted that the cylinder in the corner is also the model of vortex (Fig. 17 a) that can be observed in reality. Dust particles are being displaced leftwards at the initial flight segment already following which the second cylinder installed under the screen has its effect. Relation of d_{max} to χ in such case is shown on Fig. 18.

When a rotating suction cylinder is installed in the upper right corner (Fig. 19) of the suction unit the maximum diameter is significantly decreased. For instance, there is 10 μm decrease observed for spherical particles having the density of 3200 kg/m^3 and 32 μm decrease observed for particles having the form-factor of 6.5 and the same density.

A sinuous nature of the paths of dust particles caught by the suction cylinder should be noted which is due to the pulsating field of velocities in the suction unit: the velocity at the given point is changing regularly at the time interval equal to the suction cylinder turnaround time.

On the basis of methods of boundary integral equations [9-10], and numerical integration of the equations of motion of dust particles, there were developed a mathematical model and an algorithm for its numerical implementation and calculation program of dust and gas streams, allowing to investigate the behavior of dust particles in the technological and aspiration systems.

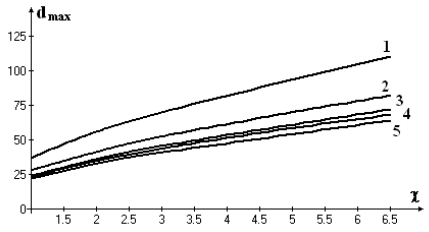

Fig. 18. Relation of d_{max} (μm) to form-factor χ during the counterclockwise rotation of the cylinder at the velocity of 8 m/s and with dust particle density of: 1 – 1400 kg/m^3; 2 – 2300 kg/m^3; 3 – 2900 kg/m^3; 4 – 3200 kg/m^3; 5 – 3500 kg/m^3

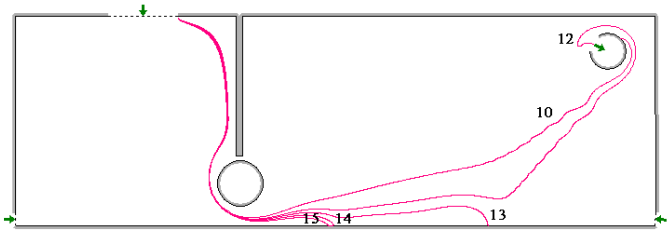

Fig. 19. Flight of dust particles when the cylinder (1.97; -1.02) is rotating counterclockwise at the velocity of 8 m/s and the suction cylinder (3.55; -0.45) is rotating counterclockwise at the velocity of 4 m/s.

The maximum diameter of the dust particles, entrained into an aspiration network of local ventilation exhausts of closed type (aspiration shelters), taking into account intake of air through leakages, essentially depends on bounding visors, availability of rotating cylinders and exhaust-cylinders. Geometrical dimensions of mechanical screens and cylinders, their location, the linear speed of rotation of the latter were determined, contributing to the reduction of the maximum diameter aspirated of dust particles on 140-200 microns.

The use into practice of aspiration shelters, equipped with exhaust - cylinder, allows to reduce undesired takeaway in an aspiration network of dust particles.

In designing of aspiration shelters with the function of dust precipitation camera is offered: To use rotating counterclockwise exhaust - cylinder; Linear speed of rotation should be high, but not contributing to the noise level; The cylinder's radius and width of the exhaust gap should be chosen as small as possible, but so that the air speed in the gap does not exceed 20 m / c; Position of exhaust-cylinder is vertically selected approximately at the center of the shelter, horizontally to the right of ventilation holes, and as close as possible to it, but so, that it does not interfere with the technological process.

Acknowledgements

The reported study was funded by RFBR according to the research project № 14-41-08005 ofi_m).

References

1. Alden, J.L. and J.M. Kane, 1982. Design of Industrial Ventilation Systems. Industrial Press, N.Y., pp: 280.

2. Sirignano, W.A, 1999. Fluid Dynamics and Transport of Droplets and Sprays. Cambridge Univ. Press, pp: 311.

3. Minko, V.A., 1981. Dust control of construction materials production processes. Voronezh: VSU Publishing, pp: 176.

4. Logachev, I.N. and K.I. Logachev, 2014. Industrial air quality and ventilation: controlling dust emissions. Boca Raton: CRC Press, pp: 417.

5. Logachev, I.N., K.I. Logachev, and O.A. Averkova, 2015. Local Exhaust Ventilation: Aerodynamic Processes and Calculations of Dust Emissions. Boca Raton: CRC Press, pp: 576.

6. Shaptala, V.G., V.V. Shaptala and A.V. Gavrilenko, 2015. Numerical Simulation of Cements-Air Mixture in Pneumochamber Pump. Bulletin of BSTU named after V.G. Shukhov, 2: 159-161.

7. Shaptala, V. G. and V. V. Shaptala, 2014. The Methods of Calculating Efficiency of Centrifugal Collectors Sticky Dust in the Production of Building Materials. Bulletin of BSTU named after V.G. Shukhov, 3: 58-62.

8. Anzheurov, N.M. and O.A. Averkova, 2008. Software for computing dusty air flows in ventilation systems. Refractories and Industrial Ceramics, 49 (3): 229-234.

9. Banerjee, P.R.,1984. Butterfield Boundary element method in applied sciences. Moscow: Mir, pp: 486.

10. Brebbia, K., G. Telles, and L Vroubel, 1987. Boundary element methods. Moscow: Mir, pp: 525.